EVALUATION OF TENSILE FRACTURE IN ASPEN USING FRACTOGRAPHIC AND THEORETICAL METHODS

John A. Akande[1] and *George H. Kyanka*

Wood Products Engineering Department
SUNY, ESF, Syracuse, NY 13210

ABSTRACT

Based on the linear elastic fracture mechanics (LEFM) concept, apparent mode I fracture toughness K_{Ic}^{LR} was calculated for unnotched aspen (*Populus tremuloides* Michx.) specimen (5 in. × 0.188 in. × 0.094 in. dimension) tested in tension parallel to grain. The purpose was to relate wood fracture toughness to average ray spacing. Observations along the longitudinal-radial plane of fracture showed the ray/fiber interface as a notable zone of crack propagation. Step-like progression of fracture lines occurred from one ray to another thus leading to an hypothesis that the average ray spacing could reasonably estimate the critical flaw dimension. Using this model, the calculated k_{Ic}^{LR} was close to available published data. In additional experiments, it was revealed that k_{Ic}^{LR} is sensitive to decay weight losses. Within 2% to 16% weight loss examined, loss of k_{Ic}^{LR} was found to be more pronounced with a brown rot fungus when compared to white rot fungi.

Keywords: Ray, fracture toughness, brown rot, white rot, decay weight loss.

INTRODUCTION

Failure of materials, including wood, are often related to their structural arrangements and associated imperfections. These materials have flaws or discontinuities which grow, sometimes to catastrophic levels, upon the application of stress. Bariska and Kucera (1985) were quick to note that wood anatomy is one most important factor affecting its failure morphology. The importance of rays in wood deformation processes has particularly generated interest among wood researchers. Keith and Côté (1968) reported that boundaries between rays and the axially oriented cells are weak points where structural changes primarily occurred. Keith (1971, 1974) defined the weak points as ray margins while Côté and Hanna (1983) described the same area as the ray/fiber interface. Côté and Hanna also recognized a stepwise fracture progression from one ray to another in red oak subjected to radial shear. To evaluate the role of the rays during wood failure, this study sets out to correlate the geometrical layout of wood rays in aspen (*Populus tremuloides*), using the linear elastic fracture mechanics concepts, to its fracture toughness. Unnotched tension parallel to grain specimens were prepared and tested to failure. Test specimens were allowed to undergo a self-initiating fracturing process with a plan that fractography will provide necessary clues to apply known theoretical assumptions. It is conceivable that failure across the necked down region of a tension parallel specimen could propagate along the LT or LR fracture modes. Fractography of an LT fracture plane is expected to reveal systematic fracturing from one growth ring to another, which was not

---

identified in this study. Fracture progression from one ray to another was, however, prominent along the longitudinal-radial plane and, for this reason, k_{Ic}^{LR} calculation was done as if the fracture pathway was coplanar. The assumption was that the theoretical stress along the shear plane is negligible. The same assumption had been made in previous studies on wood fracture toughness (Porter 1964; Debaise et al. 1966). Schniewind and Centeno (1973), Jeronimidis (1976), and Patton-Mallory and Cramer (1987) noted that very little systematic work has been published concerning the fracture toughness of wood across grain. This is felt to be due to the difficulty in explaining a situation where the introduced notch suddenly turns to fracture along the longitudinal plane. A simplified solution to this problem may be obtained by using wood fractography as demonstrated in this paper. Fracture toughness is a material property that should be sensitive to changes in wood strength. Since fungal decay is known to produce significant deterioration in wood properties, additional experiments were conducted, using the same model, to evaluate the influence of certain decay fungi on wood fracture toughness.

EXPERIMENTAL

Materials

Tension parallel to grain specimens (Fig. 1) were prepared from kiln-dried sapwood of *Populus tremuloides*. Selected specimens were all straight-grained and free of defects. These specimens were evaluated as sound wood controls and also to study the effect of *Trametes versicolor* (L.: Fr.) Pilat (SUNY ESF, 40), *Bjerkandera adusta* (Willd.: Fr.) Karst. (SUNY ESF, 58) and *Gloeophyllum trabeum* (Fr.) Murrill (SUNY ESF, 32) decay at 2%, 5%, 10% and 16% weight loss levels. Sample size for each trial was 15, and control specimens were prepared exactly the same way as their decayed counterparts, which were subsequently innoculated with test fungi and decayed for varying periods of time to achieve the desired weight loss levels. Specimens to be decayed were all moistened and sterilized prior to decay experiments.

Mechanical test

Test specimens were subjected to axial tension using a floor model TTB Instron testing machine. The loading rate was 0.05 inch per minute. To maximize gripping friction, the machine tensile test grip surfaces were faced with sandpaper. All tests were performed at the laboratory testing temperature of 72 F and 4.2% EMC. Load-deflection curves (e.g., Fig. 2) were automatically plotted on the testing machine until the first indication of failure was recorded. Usually this happened to be the maximum load (Pmax). The failure stress σ was finally calculated by dividing Pmax with the cross-sectional area of the necked-down region

$$\sigma = \text{Pmax}/0.018 \text{ psi} \tag{1}$$

Fractography

Fracture surfaces were examined with an ETEC Autoscan scanning electron microscope. The fracture surfaces were in a dry state and were merely sputter-coated with gold, using a Technics instrument, to enhance contrast and eliminate charging effects from high electron potential. Microscopic details of the fracture
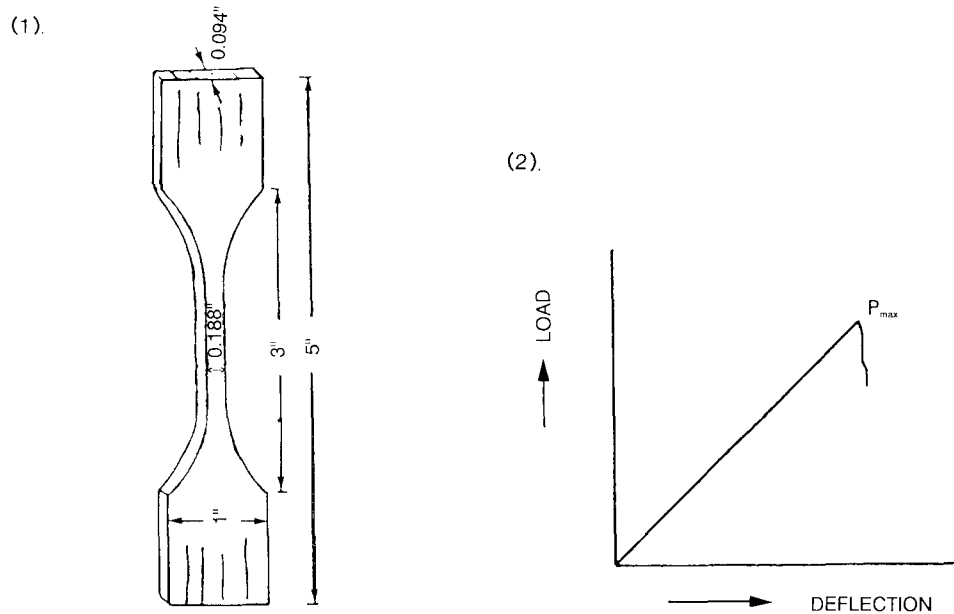
FIG. 1) Tension // grain specimen design. 2) Typical load-deflection curve in tension parallel.

surfaces were examined at 20 Kv accelerating voltage. Whenever the object on the cathode ray tube will be better demonstrated by stereo photography, adjacent pairs of photographs were taken at ±5° tilt angle.

Determination of ray spacing

An Eberbach micro-projector was utilized to enlarge microtomed (20 μm thick) cross sections from the necked down region of the tension specimens. One hundred microtomed sections were prepared and stained with sufranin-aniline. These were mounted on glass slides for closer examination under the projector, which was magnified 85 ×. The average distance between two adjacent rays was obtained by dividing the dry state width of the tension specimen necked down region by the average number of rays on this narrow cross section. An average of 26 rays were counted on each of the cross-sections examined.

Wood decay

The purified malt agar-block method (ASTM D-2017 1988a) was utilized, and the decay chambers were made from 16-ounce French square bottles. Two of the tension specimens could lie flatwise in the chamber. Fungal incubation was done at 28 C for varying time periods (9 days to 10 weeks) to obtain similar weight losses for the different fungi. Weight losses were calculated as percentages of the original oven-dry weights of the test specimens.

Specific gravity determination

After every test specimen was completely failed, five specific gravity samples were cut from each treatment category. Their specific gravities were then determined using the mercury displacement method outlined in ASTM D-2395, 1988b. The average specific gravity for each treatment group was later calculated.

THEORY

Fracture criteria

Basic linear elastic fracture mechanics concepts relate material properties, flaw size, and applied loads to the stress conditions prevailing around crack tips.

$$\sigma^2 = 2E\gamma^s/\pi a \tag{2}$$

where

$$
\begin{aligned}
E &= \text{elastic modulus,} \\
\gamma^s &= \text{surface energy,} \\
a &= \text{crack length,} \\
\sigma &= \text{fracture stress.}
\end{aligned}
$$

This equation satisfies the Griffith (1925) criterion for brittle materials and it is one of the earliest propositions concerning the LEFM concept. Irwin (1957) equated $2\gamma^s$ to G which is the strain energy release rate.

$$\sigma^2 = GE/\pi a \tag{3}$$

The quantity $(GE)^{1/2}$ is the tendency of the crack to propagate and this is recognized as the stress intensity factor K. K also represents the fracture toughness of the material which is a property useful in predicting failure loads of wood components that contain stress concentrations.

$$K = \sigma\sqrt{\pi a} \tag{4}$$

Fracture toughness K is recognized to be a function of the specimen geometry, applied stress, and the size, location and orientation of the critical flaw (Tada et al. 1973). Hence;

$$K = \sigma(\pi a)^{1/2} \cdot f(a, b, c) \tag{5}$$

after Pellicane et al. (1982).

Where

$$
\begin{aligned}
K &= \text{Fracture toughness,} \\
f &= \text{dimensionless function of specimen geometry,} \\
a &= \text{critical (effective) flaw size,} \\
b &= \text{specimen width,} \\
c &= \text{constant related to crack location in the specimen.}
\end{aligned}
$$

Since failure normally occurred at the necked down region of tension parallel to grain specimens (see Fig. 1), the specimen width can be taken as nominally constant. Also because no notch was preintroduced into specimens utilized in this study, the elements b and c in Eq. 5 may be eliminated to make the most important consideration the effective flaw size. If the stress value σ at which the critical flaw
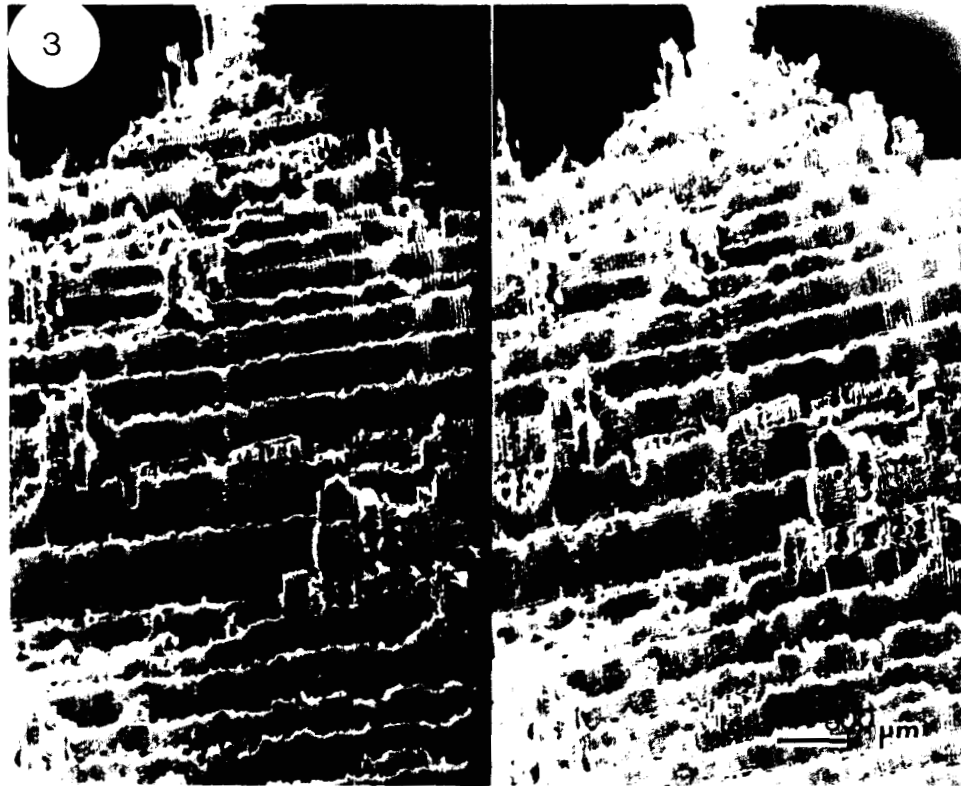
FIG. 3. Stereo scanning electron fractograph of a fractured tip of a sound specimen after failure. Notice that the fracture plane formed a step-like progression from one plane of the rays (**R**) to another. The ray/fiber interface appears to be a weak zone where shear failure occurred.

size is created is ascertained, then it is possible to calculate K. During the fracture process, it was observed that wood in tension generally behaved brittle. It was also clear that wood cells produced abrupt failure when decayed and this encouraged the belief that decayed wood will comply with LEFM assumptions. As a matter of fact, Sinclair et al. (1978) have demonstrated a positive linear relationship between fracture toughness and traditional toughness (using a Forest Products Laboratory toughness testing machine) in beetle-killed pine wood at different levels of decay.

Fractographic model

Failure in tension parallel to grain frequently occurred across grain (i.e., along the transverse plane). A close look at stereo fractographs of the fracture plane (Fig. 3) indicated that failures having shear components occurred along the ray/ fiber interfaces. When fracture lines eventually cut across the longitudinally oriented fiber cells, step-like progression of the fracture plane resulted. The fracture line obviously passed through sloping planes, across the fiber cells (see Figs. 4 and 5a, b), until it becomes full (effective) crack length between rays. By the time the fracture line moved from one ray to another in sound wood, an average angle of approximately 45° (estimated visually) was projected to the transverse plane.

FIG. 4. Scanning electron fractograph showing a step-like fracture pattern from plane (A) of ray R to another plane (B) in sound wood. The "step angle" was steep. tw indicates transwall failure of the longitudinally oriented fibers and vessels. Note that the cell lumens are generally opened during transwall failures.

This step angle appeared to be influenced by the failure angle of individual cells illustrated in Fig. 6. After examining several fractographs, it was apparent that microflaws exist in wood. Upon the application of stress, small flaws within individual fibers would coalesce to form larger cracks whose length becomes critical to failure at the measured distance between rays. The critical crack is equivalent to the ray spacings and is analogous to the voids between butt joints in laminated wood beams. The stress condition at the periphery of the crack tip is essential to an understanding of the failure process in wood which contained a defined locus of stress concentration like the ray/fiber interface. Any crack tip bordering these zones would propagate in an unstable fashion.

The fracture behavior of wood cells can be analyzed by taking a technique from Williams and Birch (1976), who showed that shear failure is less significant when analyzing mixed mode fracture in anisotropic media loaded in tension and that the fracture behavior can be evaluated as pure mode I. A situation where cracks turned to run parallel to the grain direction could be analyzed as pure shear mode along the ray/fiber interface. The theoretical stress on this plane of fracture equals zero, and the true fracture stress is considered to be resisted by the longitudinally oriented cells. Consequently, K_{II} and K_{III} becomes negligible while K_I calculation employs the numerical flaw size prior to unstable crack propagation along ray/fiber interface. Since shear failure is not considered significant under tension
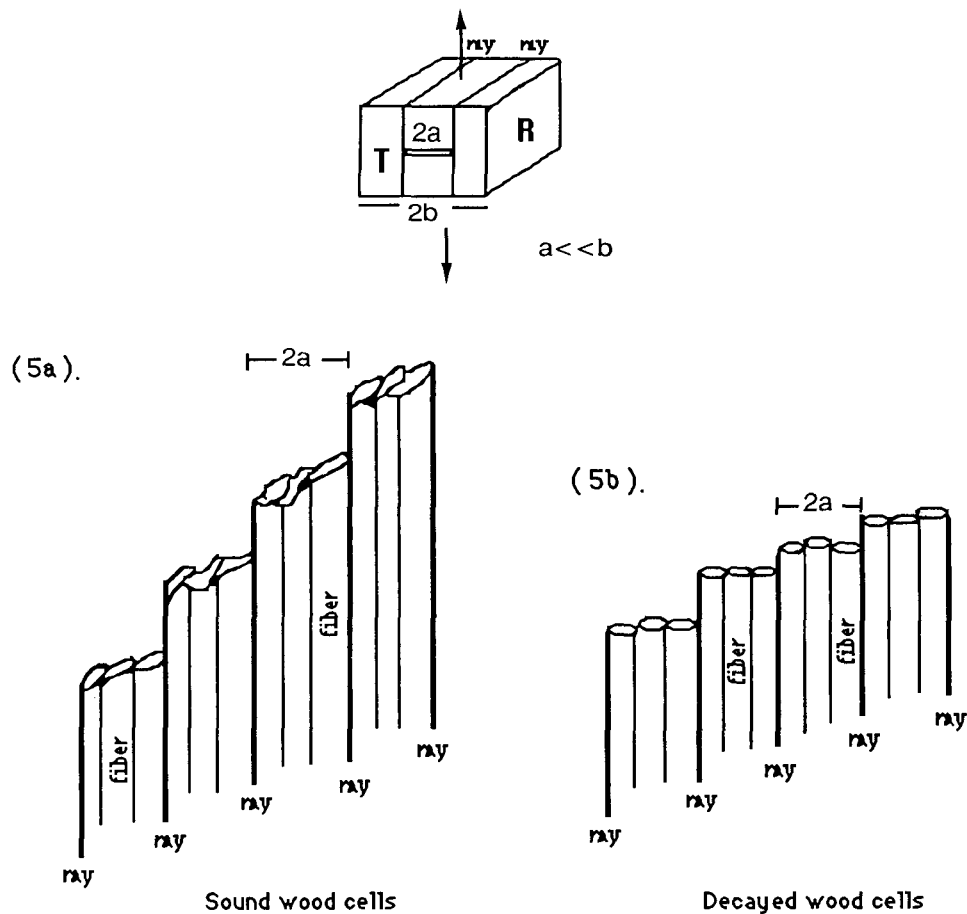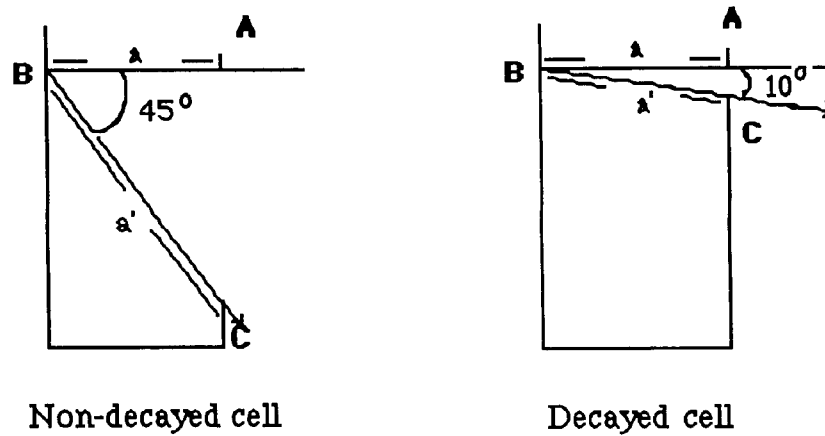
FIG. 5. Step-like fracture seen from tangential-longitudinal plane.

parallel to grain, K_I calculation can be done as if the critical crack had propagated in a coplanar fashion.

With regard to wood decay, microscopic evidence in this research (Fig. 7) indicated that fracture jumps also occurred from ray to ray, but many of the longitudinally oriented cells offered little or no resistance and, therefore, broke abruptly at low angles (about 10° or lower) to the transverse plane (see Fig. 8).

The assumption that the average spacing between rays corresponds to the critical flaw dimension is similar to the assumption made by Jung and Murphy (1983) while examining the effect of butt joints on fracture behavior of parallel laminated veneer members. The ply thickness was assumed by these workers to correspond to the critical flaw size in their calculation of fracture toughness. This same assumption was made by Smith and Penny (1980) while analyzing the fracture behavior of butt-jointed laminated wood beams. Figure 9a and b show the similarity between Jung and Murphy's model and the present model. To calculate the apparent fracture toughness in butt-jointed laminated wood, Jung and Murphy (1983) used the following equation

$$K_I = \sigma\sqrt{\pi t} \cdot F(d/t)g(dm/t) \tag{6}$$

Non-decayed cell   Decayed cell

N.B.   BC is the fracture plane and $\angle$ **ABC** is the reference angle.

FIG. 6.   Idealized diagram showing the 'step angles' to failure on individual wood cell.

FIG. 7.   Scanning electron fractograph showing a longitudinal-radial fracture plane in wood decayed by *Gloeophyllum trabeum* to 5% weight loss. Notice a step-like progression of the fracture plane. The longitudinally oriented fibers (f) and vessels (V) failed in an abrupt transwall (tw) fashion at angles almost parallel to the transverse plane. hy shows hypha in vessel lumen. R indicates ray cell.

FIG. 8. Scanning electron fractograph showing a longitudinal-radial fracture plane in wood decayed by *Bjerkandera adusta* to 10% weight loss. Observe how the ray cell (R) was degraded (arrows) and how abrupt transwall fracture (tw) of vessels (V) and fibers (F) occurred at angles almost perpendicular to the grain direction.
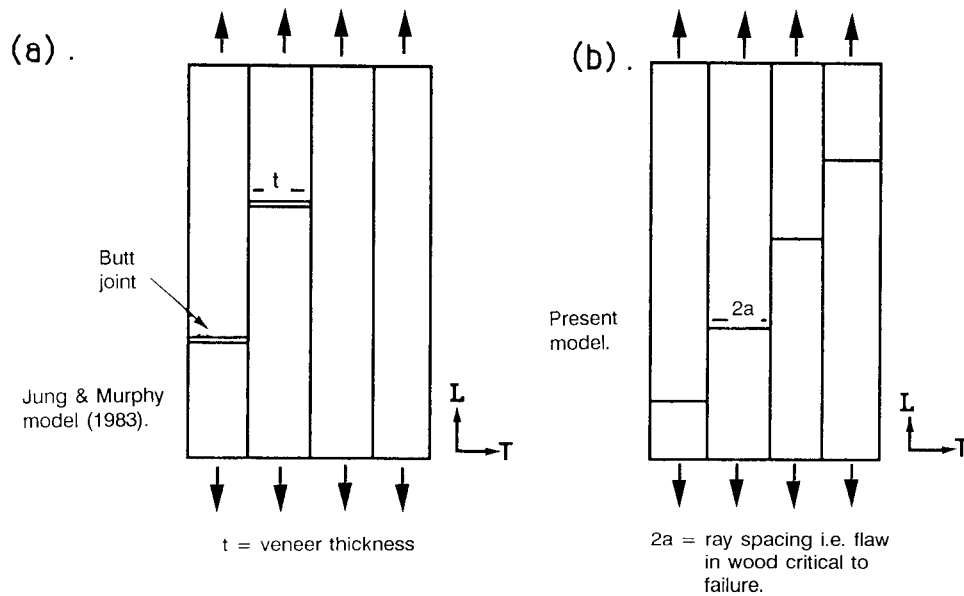

FIG. 9. Models for fracture toughness determination.

where

σ = tensile stress,

t = veneer thickness (synonymous with ray spacing in this investigation),

d = specimen width,

m = butt joint spacing,

F = correction factor relating K to t/d ratio for an isotopic material (Tada et al. 1973),

g = function to correct for interaction of edge butt joint and butt joint in the next adjacent lamina.

The function F(d/t)g(dm/t) is similar to f(a, b, c) in Eq. 5 and it relates to crack geometry, location, and size. The value of these functions for a body loaded in tension and containing a central crack is always close to unity (see Pellicane et al. 1982). In a situation where fractography has already provided essential information about the geometry, location, and size of critical flaws, Eq. 6 can be condensed to $K_I = \sigma\sqrt{\pi t}$, which is the same as Eq. 4, except that t now becomes the critical crack length or ray spacing on the fractographs.

CALCULATION OF K_{Ic}^{LR}

As a first order approximation, the load needed to calculate K_{Ic} corresponds to the first indication of instability on the load-deflection diagram. As already indicated, this was Pmax in many of the instances and its average value dropped for each of the treatment groups as decay progressed. The average spacing between rays is also felt to be equivalent to a critical crack embedded in wood. It was therefore equated to 2a. Jung and Murphy (1983) already demonstrated that K_{Ic} may be insensitive to the exact crack location as long as the crack remains in the material interior and perpendicular to the line of applied uniaxial stress.

$$2a = 0.0072 \text{ in.} \qquad \therefore a = 0.0036 \text{ in.} \tag{7}$$

A close look at the fracture line across the longitudinally oriented cells (fig. 4) showed that the fracture line is not exactly perpendicular to the fiber axis. In other words, the crack length is somewhat different from a, and the effective crack length a' = a/cos B (see Fig. 6) where B is the "step angle" across the longitudinally oriented cells. Thus, for sound wood where B $\approx$ 45°, cos B = 0.707 and a' = 0.0051 in. This same dimension can be taken for 2% weight loss since fractographic evidence (Fig. 10) showed that the wood cells still remained sound. Beyond 2% weight loss, the worst flaw theory will be assumed because cells that broke abruptly from decay were likely to influence fracture pathway. For decayed cells, an angle of failure B $\approx$ 10° will be assumed (see Fig. 6). Cos B = 0.985, therefore a' = 0.0037 in.

The fracture stress σ psi was calculated on force per unit nominal cross sectional area. The stress values and corresponding fracture toughness values obtained, by using Eq. 4 are presented in Table 1.

Effect of changing specific gravity

Wood specific gravity changes with decay. It will not be correct because of this change to calculate the estimated true fracture stress based on a nominal cross-

FIG. 10. Scanning electron fractograph of a longitudinal-radial fracture plane in wood decayed by *Trametes versicolor* to 2% weight loss. The step angles of failure across the longitudinally oriented cells were steep just like that of sound wood.

sectional area obtained for sound wood specimens. The true area of the specimen cross section is bound to change as the wood specific gravity drops with decay. The estimated true fracture stress σ^* was calculated as force per unit area of the actual cell-wall substance present.

$$\sigma^*\text{psi} = P_{max}/A_w \qquad (8)$$

where

$$A_w = \text{area of cell wall substance}$$

The actual area of cell wall substance was calculated based on this eq. from Siau (1971).

$$V_a = 1 - S.G(0.667 + 0.01M) \qquad (9)$$

TABLE 1. *Nominal fracture stress σ psi and (corresponding K_{Ic}^{LR} psi $\sqrt{in.}$).*

% Wt. loss	Sound wood	T. versicolor	B. adusta	G. trabeum
0	12,362 (1,564)	—	—	—
2	—	12,177 (1,541)	11,806 (1,494)	8,097 (1,025)
5	—	11,942 (1,287)	10,965 (1,182)	6,552 (706)
10	—	10,730 (1,157)	9,828 (1,059)	5,192 (560)
16	—	8,011 (863)	8,072 (870)	4,351 (469)

TABLE 2.   *Wood specific gravity SG and (corresponding areas of cell-wall substance A_w in.²).*

% Wt. loss	Sound wood	T. versicolor	B. adusta	G. trabeum
0	0.447	—	—	—
	(0.00537)	—	—	—
2	—	0.440	0.429	0.440
	—	(0.00530)	(0.00515)	(0.00530)
5	—	0.430	0.400	0.410
	—	(0.00520)	(0.00480)	(0.00490)
10	—	0.392	0.370	0.350
	—	(0.00470)	(0.00440)	(0.00420)
16	—	0.299	0.320	0.330
	—	(0.00360)	(0.00380)	(0.00400)

where

V_a = fractional void volume,

S.G = specific gravity at moisture content M

It was assumed in deriving Eq. 9 that the specific gravity of water = 1 and that the specific gravity of cell-wall substance = 1.5. Since the wood specimens tested in this work were all at oven-dry conditions, M ≈ 0. Average S.G of the test samples was measured and the results are presented in Table 2.

At oven-dry conditions,

$$V_a = 1 - 0.667 S.G \tag{10}$$

where 0.667S.G is the fractional wood volume V_w, same as the fractional volume of wood substance which can take a wide range of values from 0 to 1. Once V_w is known by using S.G at oven-dry conditions, the area of cell wall substance A_w can be calculated.

$$A_w = 0.018 \times V_w \tag{11}$$

where 0.018 in² as previously mentioned is the nominal cross sectional area of the test specimen.

TABLE 3.   *Mean load at failure P_{max} lb, standard deviation, and (true stress σ*psi calculated from the average load values).[1]*

% Weight loss	Sound wood	T. versicolor	B. adusta	G. trabeum
0	222.5 ± 38.6	—	—	—
	(41,434)	—	—	—
2	—	219.2 ± 33.9	212.5 ± 38.5	145.8 ± 34.7
	—	(41,359)	(41,262)	(27,509)
5	—	215.0 ± 23.6	197.4 ± 33.2	117.9 ± 42.1
	—	(41,346)	(41,125)	(24,061)
10	—	193.0 ± 38.4	176.9 ± 30.7	93.5 ± 24.5
	—	(41,064)	(40,205)	(22,262)
16	—	144.2 ± 38.9	145.3 ± 36.2	78.3 ± 22.6
	—	(40,056)	(38,237)	(19,575)

[1] Average value obtained from a sample size of 15 for each test condition.

TABLE 4. $K^*_{Ic}{}^{LR}$ *psi* $\sqrt{in.}$ *and its (log transformation).*

% Wt. loss	Sound wood	*T. versicolor*	*B. adusta*	*G. trabeum*
0	5,243	—	—	—
	(3.720)	—	—	—
2	—	5,234	5,222	3,481
	—	(3.719)	(3.718)	(3.542)
5	—	4,457	4,433	2,593
	—	(3.649)	(3.647)	(3.414)
10	—	4,426	4,334	2,400
	—	(3.646)	(3.637)	(3.380)
16	—	4,318	4,121	2,110
	—	(3.635)	(3.615)	(3.324)

$$A_w = 0.018 \times 0.667S.G = 0.012S.G \tag{12}$$

The area of cell-wall substance A_w calculated for each of these S.G values is also given in Table 2. The estimated true fracture stress

$$\sigma^*psi = Pmax/0.012S.G \tag{13}$$

Results obtained for the true fracture stress σ^*psi at different decay weight loss levels are presented in Table 3 and the apparent fracture toughness values $K^*_{Ic}{}^{LR}$ obtained by using the estimated true stress data are given in Table 4. Figure 11 shows the relationship obtained between Log $K_{Ic}{}^{LR}$ and percent weight loss with decay. As weight loss increased due to fungal decay, the observed resistance to fracture dropped as expected.
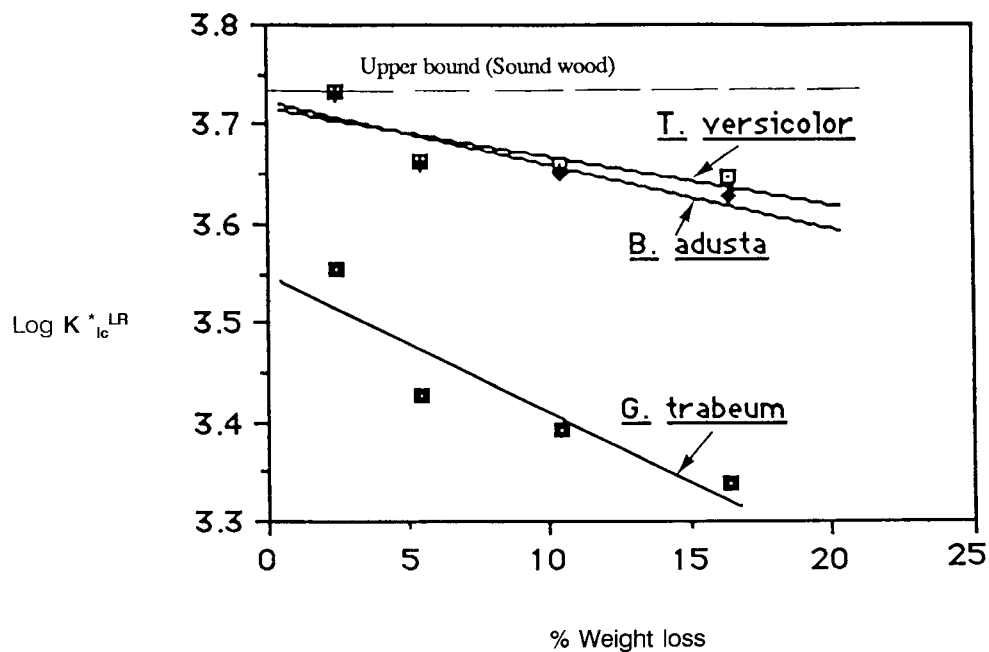

% Weight loss

FIG. 11. $K^*_{Ic}{}^{LR}$ as a function of decay weight losses.

TABLE 5. *Reported K_{Ic}^{LR} data for woods.*

Source	Wood specimen	Mean K_{Ic}^{LR} psi $\sqrt{in.}$	Moisture content %
Schniewind & Centeno (1973)	Douglas fir (edge notched beam) (static bending)	2,450	12
Murphy (1978)	Douglas fir (slit notched beam) (static bending)	1,466	11
Present study	Aspen (tension parallel)	1,564	Oven-dried

Letting x represent the percentage weight loss, the least square regression fits for the different fungal treatment are given as follows:

$$\text{Trametes versicolor:} \quad \text{Log } K^*{}_{Ic}^{LR} = 3.7026 - 0.0049x \tag{14}$$

$$\text{Bjerkandera adusta:} \quad \text{Log } K^*{}_{Ic}^{LR} = 3.7061 - 0.0063x \tag{15}$$

$$\text{Gloeophyllum trabeum:} \quad \text{Log } K^*{}_{Ic}^{LR} = 3.5289 - 0.0138x. \tag{16}$$

DISCUSSION AND CONCLUSIONS

Relatively few data exist on LR and LT fracture modes in wood because of the difficulty in monitoring crack tip displacements which often get arrested or turn abruptly to cause splitting along the grain (Schniewind and Centeno 1973). In this study, a reasonable estimate of the amount of energy absorbed in an LR mode of fracture across grain was obtained by relating fractographic evidences to experimental stress data. Results obtained by using nominal fracture stress in this work are close to available data for other woods (see Table 5). It is felt that any error involved in calculating the K_{Ic}^{LR} value is marginal and may be related to the visual selection of step angles from one ray to another.

Comparison of the fracture surfaces with the fracture toughness values indicates that the geometry of the surface profile is important to an analysis of the energy absorbed during wood fracture. When the fracture plane is relatively flat due to abrupt breakage of cells in decayed wood, K_{Ic}^{LR} value falls. For a jagged fracture plane resulting from angular failures across sound wood cells, a tougher fracture energy was encountered. The declining trend in fracture toughness with decay weight loss is similar to that reported with increasing loss of specific gravity by Sinclair et al. (1978). Attempts were not made to calculate fracture toughness along other modes of crack propagation, in this work, because the fracture stresses leading to failure in these modes were not at our disposal. Generally, crack produced in tension often follows a steep angle across sound wood fibers until its tip reaches the weak interface between ray and fiber cells where rapid crack propagation occurred. The region of the rays was also identified to be weak in decayed wood but the step angles across the longitudinally oriented cells were relatively flat compared to that in sound wood. Based on fractographic evidence which projected the ray/fiber interface as a weak region, it is postulated that the spacing between rays can be important in obtaining fracture toughness values for wood. The step-like progression of fracture from one ray to another also supports this

view. Before this postulate is, however, accepted for engineering application, further research is recommended to calculate K_{Ic}^{LR} values for different wood species (using the distance between rays as the critical flaw dimension) so that the results can be compared to published data. In doing this, it is suggested that wood samples be selected from specified locations in the log. This is felt to be important because the spacing between rays may widen from pith to bark in some species and this can influence the fracture toughness values.

REFERENCES

AMERICAN SOCIETY FOR TESTING AND MATERIALS (ASTM). 1988a. Standard method of accelerated laboratory test of natural decay resistance of woods. D 2017-81/86. Annual book of ASTM standards. Construction. Section 4, vol. 04.09 Wood, Philadelphia, PA, pp. 323–326.

―――. 1988b. Standard test methods for specific gravity of wood and wood-base materials. D 2395-69/77. Annual book of ASTM standards. Construction. Section 4, vol. 04.09 Wood, Philadelphia, PA, pp. 359–366.

BARISKA, M., AND L. J. KUCERA. 1985. On the fracture morphology in wood. Part 2: Macroscopic deformations upon ultimate axial compression in wood. Wood Sci. Technol. 19:19–34.

CÔTÉ, W. A., AND R. B. HANNA. 1983. Ultrastructural characteristics of wood fracture surfaces. Wood Fiber Sci. 15(2):135–163.

DEBAISE, G. R., A. W. PORTER, AND R. E. PENTONEY. 1966. Morphology and mechanics of wood fracture. Materials Res. Stand. 6:493–499.

GRIFFITH, A. A. 1925. Proceeding of the 1st International Congress for Applied Mechanics. Delft (Waltman). 55 pp.

IRWIN, G. P. 1957. Analysis of stresses and strains near the end of a crack traversing a plate. J. Appl. Mech. 57(22):361–364.

JERONIMIDIS, G. 1976. The fracture of wood in relation to its structure. Leiden Botanical Service 3: 253–265.

JUNG, J., AND J. F. MURPHY. 1983. An investigation of the fracture of butt joints in parallel-laminated veneer 1. Wood Fiber Sci. 15(2):116–134.

KEITH, C. T. 1971. The anatomy of compression failure in relation to creep-inducing stresses. Wood Science 4:71–82.

―――. 1974. Longitudinal compressive creep and failure development in white spruce compression wood. Wood Science 7:1–12.

―――, AND W. A. CÔTÉ. 1968. Microscopic characterization of slip lines and compression failures in wood cell walls. Forest Prod. J. 18(3):67–74.

MURPHY, J. F. 1978. Using fracture mechanics to predict failure in notched wood beams. Proceedings, 1st International Conference on Wood Fracture. Banff, Alberta, pp. 159–173.

PATTON-MALLORY, M., AND S. M. CRAMER. 1987. Fracture mechanics: A tool for predicting wood components strength. Forest Prod. J. 37(7/8):39–47.

PELLICANE, P. J., J. BODIG, AND J. R. GOODMAN. 1982. Simulation of the tensile strength-fracture toughness relationship. Wood Science 14(4):168–177.

PORTER, A. W. 1964. On the mechanics of fracture in wood. Forest Prod. J. 13:325–331.

SCHNIEWIND, A. P., AND J. C. CENTENO. 1973. Fracture toughness and duration of load factor 1. Six principal systems of crack propagation and duration factor for crack propagating parallel to grain. Wood Fiber 5(2):152–159.

SIAU, J. F. 1971. Flow in wood. Syracuse University Press, Syracuse, NY, 131 pp.

SINCLAIR, S. A., G. IFJU, AND J. A. JOHNSON. 1978. Changes in toughness of wood from beetle-killed shortleaf pine. Forest Prod. J. 28(7):44–47.

SMITH, F. W., AND D. T. PENNY. 1980. Fracture mechanics analysis of butt joints in laminated wood beams. Wood Science 12(4):227–235.

TADA, H., P. C. PARIS, AND G. R. IRWIN (ED.). 1973. Stress analysis of cracks handbook. Del Research Corp. Hellertown, PA.

WILLIAMS, J. G., AND M. W. BIRCH. 1976. Mixed mode fracture in anisotropic media. ASTM, 1916 Race Str. Phil., PA 19103. Technical Bulletin 601:125–137.